Impact of potential engine malfunctions on fuel consumption and gaseous emissions of a Euro VI diesel truck

Yuhan Huang[1,*], Elvin C.Y. Ng[2,3], Yat-shing Yam[4], Casey K.C. Lee[4], Nic C. Surawski[1], Wai-chuen Mok[1], Bruce Organ[1,3], John L. Zhou[1,*], Edward F.C. Chan[1,5]

[1] School of Civil and Environmental Engineering, University of Technology Sydney, NSW 2007, Australia

[2] School of Mechanical and Mechatronic Engineering, University of Technology Sydney, NSW 2007, Australia

[3] Jockey Club Heavy Vehicle Emissions Testing and Research Centre, Vocational Training Council, Hong Kong

[4] Environmental Protection Department, Hong Kong Special Administrative Region Government, Hong Kong

[5] Technological and Higher Education Institute of Hong Kong, Vocational Training Council, Hong Kong

Corresponding authors:

Prof John L. Zhou, Email: junliang.zhou@uts.edu.au

Dr Yuhan Huang, Email: yuhan.huang@uts.edu.au

Abstract

Although new vehicles are designed to comply with specific emission regulations, their in-service performance would not necessarily achieve them due to wear-and-tear and improper maintenance of engine components as well as tampering or failure of the engine control and exhaust after-treatment systems. However, there is a lack of knowledge on how much these potential malfunctions affect vehicle performance. Therefore, this study was conducted to simulate the effect of some common engine malfunctions on the fuel consumption and gaseous emissions of a 16-tonne Euro VI diesel truck using transient chassis dynamometer testing. The simulated malfunctions included those that would commonly occur in the intake, fuel injection, exhaust after-treatment and other systems. The results showed that all malfunctions increased fuel consumption except for the malfunction of EGR fully closed which reduced fuel consumption by 31%. The biggest increases in fuel consumption were caused by malfunctions in the intake system (16%-43%), followed by the exhaust after-treatment (6%-30%), fuel injection (4%-24%) and other systems (6%-11%). Regarding pollutant emissions, the effect of engine malfunctions on HC and CO emissions was insignificant, which remained unchanged or even reduced for most cases. An exception was EGR fully open which increased HC and CO emissions by 3.4 and 11.2 times, respectively. Contrary to HC and CO emissions, NO emissions were significantly increased by malfunctions. The largest increases in NO emissions were caused by malfunctions in the after-treatment system, ranging from 38% (SCR) to 16.1 times (DPF pressure sensor). Malfunctions in the fuel injection system (24%-12.6 times) and intercooler (4.4-6.0 times) could also increase NO emissions markedly. This study demonstrated clearly the significance of having properly functioning engine control and exhaust after-treatment systems to achieve the required performance of fuel consumption and pollutant emissions.

Keywords: Intake system; Fuel injection; Exhaust after-treatment; Malfunctions simulation; Fuel consumption; Gaseous emissions

Highlights

- Effect of engine malfunctions on performance of a Euro VI diesel truck was simulated.
- All malfunctions increased fuel consumption except for EGR fully closed.
- Effect of malfunctions on HC and CO emissions was insignificant.
- NO emissions could be increased by up to 16.1 times by after-treatment system faults.
- Proper functioning of engine control systems is crucial to achieve the design standards.

Abbreviations:

CRDI: Common-rail direct injection

DOC: Diesel oxidation catalyst

DPF: Diesel particulate filter

ECU: Engine control unit

EGR: Exhaust gas recirculation

HKEPD: Hong Kong Environmental Protection Department

IDI: Indirect injection

I/M: Inspection and maintenance

MWTD: Medium Goods Vehicle Working Test Drive

SCR: Selective catalytic reduction

1. Introduction

Heavy-duty diesel vehicles are widely used for commercial road transport due to their high thermal efficiency. Although they represent a relatively small share (< 5%) of the global on-road vehicles, they produce significant percentages (40-60%) of the total NO_x and PM emissions [1-3]. Automotive emission standards have become increasingly stringent to address this issue. For example, the transition from Euro V to Euro VI required large diesel engines to reduce the NO_x and PM emission limits significantly by 80% (from 2.0 to 0.4 g/kW-h) and 50% (from 0.02 to 0.01 g/kW-h) in steady-state testing and by 77% (from 2.0 to 0.46 g/kW-h) and 67% (from 0.03 to 0.01 g/kW-h) in transient testing, respectively [4]. In addition, real-driving emissions (RDE) test has also been adopted for type approval to mitigate the significant gap between laboratory and on-road emissions performance [4-6]. These lead the automotive industry to adopt more complex and reliable engine control and exhaust after-treatment systems to meet the ever stricter regulations. Consequently, fuel consumption and emissions performance of modern diesel vehicles are greatly dependent on the precise control and correct functioning of the engine control and exhaust after-treatment systems [7].

Extensive studies have been conducted to investigate the effectiveness and significance of individual engine technologies on fuel economy and emissions performance, such as turbocharging [8, 9], injection pressure [10] and timing [11-13], exhaust gas recirculation (EGR) [12-14], diesel particulate filter (DPF) [15], diesel oxidation catalyst (DOC) [16, 17] and selective catalytic reduction (SCR) [18, 19]. Although all the new vehicles are designed to comply with specific emission regulations, their in-service performance would not achieve the same standards due to deterioration, improper maintenance, tampering or failure of the engine control and exhaust after-treatment systems [20]. However, there is a lack of knowledge on how malfunctions in one or more of the above engine technologies could affect vehicle performance, considering that modern diesel vehicles are a complex assembly of multiple engine and emission control devices.

Chase et al. [21] tested the engine performance of a heavy duty truck after a 322000-km operational demonstration using a diesel-biodiesel blend. They observed a significant increase in transient PM emissions but a decrease in NO_x emissions, which were attributed to the decreased injection pressure and delayed fuel injection due to normal engine wear during the long-haul operation. McCormick et al. [22] compared the smoke opacity and regulated pollutant emissions of 20 heavy duty diesel vehicles emitting visible smoke before and after repairs. The results showed significant decreases in smoke opacity and PM emissions, but increases in NO_x emissions after repairs that targeted visible smoke emissions. However, the above two studies are relatively old, with test vehicles manufactured before 1996. Consequently, their engine combustion and exhaust after-treatment technologies would be different to those of modern diesel vehicles. For example, older small diesel engines usually used mechanical indirect injection (IDI) system with a pre-combustion chamber [23] and few exhaust after-treatment devices were used, while almost all modern diesel engines are commonly equipped with common-rail direct injection (CRDI) system plus various exhaust after-treatment devices such as EGR, DPF, SCR and DOC. Kowalski [24] simulated the effect of two malfunctions in the mechanical fuel pump, namely delayed injection timing and fuel leakages, on a marine diesel engine under constant speed conditions. The results showed that both malfunctions caused very small changes in thermodynamic parameters of the engine, but caused remarkable increases in CO_2 emissions and decreases in NO_x emissions. CO emissions were increased by injection delay only at high loads and were increased significantly by fuel leakage at medium loads.

As reviewed above, very few studies have been conducted to investigate the effect of diesel engine malfunctions on fuel consumption and emissions, although it has been proven that proper functioning of the engine and emission control system is crucial for achieving the expected engine performance [21, 22, 24]. In addition, existing papers mostly only studied malfunctions occurred in one engine device (e.g. fuel pump [24]). However, modern diesel vehicles are now equipped with complex engine management and exhaust after-treatment systems, making it challenging for the motor maintenance and repair industry to diagnose and repair the emission-related faults [7].

A comprehensive study on a modern diesel vehicle is of great importance to help the motor repair industry identify and repair the emission-related faults quickly. Motor repairs fall within the scope of the Hong Kong Environmental Protection Department (HKEPD) on-road remote sensing program that identifies high-emitting vehicles for enforcement. The HKEPD has made discernible improvement to roadside air quality by adopting the on-road remote sensing technology to tackle the excess emissions from petrol and liquefied petroleum gas vehicles [25]. To further improve roadside air quality, it is developing an on-road remote sensing enforcement program for diesel vehicles [5]. On-road remote sensing is an effective and economic tool for use in automotive emissions control. It is non-intrusive and can measure the emissions of a passing vehicle in a half second. Therefore, it can measure the emissions of a large number of vehicles at a relatively low cost. The remote sensing emission data can be used to screen out high-emitting vehicles for repair or deregistration, which is essential for implementing targeted emission control programs such as inspection and maintenance (I/M) [26]. An effective I/M program using remote sensing can capture a large portion of the fleet and a significant number of high-emitting diesel vehicles would be identified for repairs [5].

A prerequisite for introducing a diesel I/M program is that vehicle mechanics have the requisite knowledge to effectively identify and repair emission-related faults of modern diesel vehicles. Therefore, this study is conducted to understand how various engine malfunctions of a modern diesel truck would influence the fuel consumption and gaseous emissions performance. The test vehicle is a Euro VI heavy duty diesel truck equipped with common emission reduction technologies. 16 faults that would likely occurred in the intake, fuel injection and exhaust after-treatment systems are simulated using a chassis dynamometer.

2. Experimental section

2.1. Test rig and procedures

Table 1 gives specifications of the test vehicle. The test vehicle was a Scania G280 manual transmission truck. The truck had a reference mass of 10 tonnes and a maximum mass of 16 tonnes. It was equipped with a 9.3 L turbocharged diesel engine. The compression ratio was 18:1. The rated maximum power and torque outputs were 206 kW @ 1900 rpm and 1400 Nm @ 1000-1350 rpm, respectively. To meet the Euro VI standard, the engine was equipped with various emissions reduction technologies, including high-pressure CRDI, turbocharger, EGR, SCR, DOC and DPF.

Table 1. Specifications of the test vehicle.

Vehicle model	Scania G280, manual gearbox, rear wheel drive
Manufacture year	2013 (Euro VI)
Reference/maximum mass	10160/16000 kg
Engine type	Scania Turbo diesel engine
Fuel injection system	High-pressure (500-2400 bar) CRDI
Displacement	9.3 Litres
Number of cylinders	5, in-line
Compression ratio	18 : 1
Bore × stroke	130 × 140 mm
Rated maximum power	206 kW @ 1900 rpm
Rated maximum torque	1400 Nm @ 1000-1350 rpm
Exhaust after-treatment	EGR, DOC, SCR and DPF

(a)

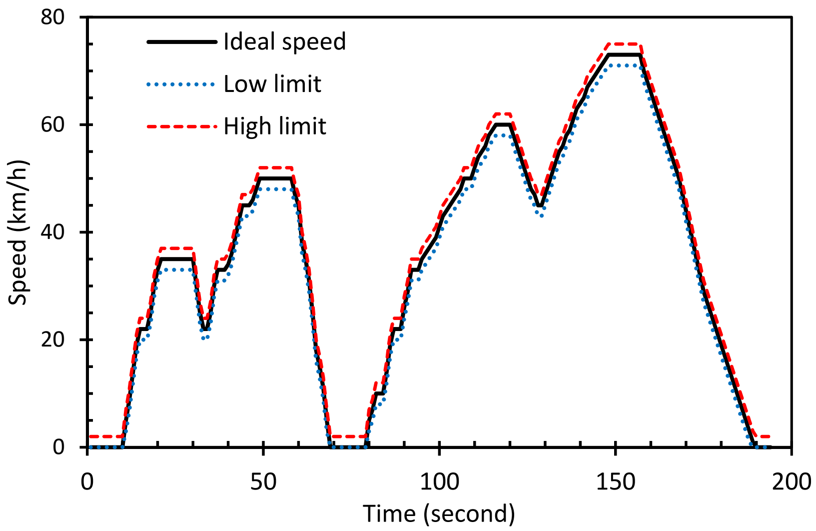

(b)

Fig. 1. Chassis dynamometer testing rig (a) and the MWTD cycle (b).

The experiments were conducted in the Jockey Club Heavy Vehicle Emissions Testing and Research Centre in Hong Kong, where the chassis dynamometer and emission analysers were certified to European standards. Fig. 1(a) shows the setup of the chassis dynamometer and test cycle. The test vehicle was tied down on a 17.8-inch-roller Mustang Dynamometer. For each experimental condition, the vehicle was driven under the Medium Goods Vehicle Working Test Drive (MWTD) cycle conditions, which was developed for commercial vehicles above 5.5 tonnes based on real-driving conditions measured on Hong Kong roads. As shown in Fig. 1(b), MWTD cycle is a 195-second transient chassis dynamometer test. The total cycle distance is 1927 m and the maximum speed is 73 km/h. The speed tolerance is ± 2 km/h and the time tolerance is ± 1 second. Each experiment was repeated three times to estimate measurement uncertainties.

A Sensors Inc. Exhaust Flow Meter High Speed (EFM HS) was used to measure the exhaust mass flow rate. An EMS 5002/5003 gas analyser was used to measure the gas concentrations of O_2, CO_2, CO, HC and NO. CO_2, CO and HC were measured by non-dispersive infrared (NDIR) with a solid state sensor; and NO and O_2 were measured by an electro-chemical cell. The accuracy specifications were 0.1% for O_2, 0.3% for CO_2, 0.06% for CO, 4 ppm for HC and 25 ppm for NO. The exhaust flow rate and emission concentrations were measured and recorded at 1 Hz. The emission factors in *g/km* for each test cycle were calculated using the method defined in the Regulation No 83 of the Economic Commission for Europe of the United Nations [27]. The fuel consumption rate in *L/100 km* was calculated based on the principle of carbon balance and using a diesel density of 832 *g/L*.

2.2. Simulation of malfunctions

The vehicle was firstly tested with all the engine and emission control systems functioning properly, which was used as the baseline for comparison. Then, 16 common engine malfunctions were individually investigated, including those would likely occur in the intake (a-c), fuel injection (d-h), exhaust after-treatment (i-n) and other (o-p) systems. A malfunction was simulated by either disconnecting, mechanically disabling or removing the relevant engine part or emission control device. The functions and simulation methods of each device are described as follows:

2.2.1. Intake system

a) EGR fully open/closed

The EGR valve controls the amount of exhaust gas recirculated into the intake manifold, which dilutes the intake charge oxygen and reduces the combustion temperature to reduce NO_x formation. The EGR valve is controlled by the Engine Control Unit (ECU) and is actuated by a pneumatically controlled valve to open or close. In this study, EGR fully open was simulated by installing an actuator fixed in the open position and EGR fully closed was simulated by disconnecting the pneumatic air supply for the closed position (Fig. S1). During the experiments, rough idling would be observed if EGR was stuck fully open. On the other hand, EGR fully closed would lead to higher combustion temperature, NO emissions and pinging. This is dependent upon the capability of the ECU and the feedback systems installed in each vehicle to detect EGR malfunctions and counter-act. For a Euro 6/VI system, other control measures such as SCR and a power limit can be undertaken to improve engine performance and emissions.

b) Intercooler air leakage/no air cooling

An intercooler cools the compressed air from the turbocharger and increases the air density before entering the combustion chamber, allowing for better combustion and higher power generation. Air leakage was simulated by disconnecting the hose of the intercooler (Fig. S2). No air cooling was simulated by installing an intercooler with damaged cooling fins so air crossflow was minimised and did not allow for any effective cooling of the intake air to be achieved.

c) Air filter blockage

An air filter removes debris, dust and particles from the intake air to provide clean air for combustion. If not installed, the contaminants could potentially damage the engine cylinders and reduce the combustion efficiency. Simulation of blockage was achieved by acquiring a used and blocked air filter (Fig. S3). A blocked air filter reduces the volumetric efficiency of the engine and increases the pumping loss, leading to higher fuel consumption.

2.2.2. Injection system

d) Fuel rail blockage

The fuel rail distributes diesel to each of the fuel injectors at a regulated pressure for injecting into the combustion chamber. Fuel rail blockage was simulated by installing a ball valve to restrict/reduce the fuel flow rate. The valve handle was set at 75° (0° refers to fully open, Fig. S4). Rough idling or running may occur if the fuel injection is inconsistent.

e) Common rail pressure sensor

A pressure sensor continuously monitors the pressure in the fuel rail, providing a feedback signal to the fuel pressure regulator to maintain the required minimum rail pressure and to ensure consistent fuel delivery. The malfunction was simulated by disconnecting the fuel pressure sensor (Fig. S5). In this state, the fuel pressure is regulated by a mechanical pressure-relief valve. When this occurs, the engine will be able to run but it may result in greater variance in fuel injection and possible over supply of fuel to the engine.

f) Fuel pump pressure sensor

The fuel pump pressurises and supplies diesel fuel to the fuel rail and then injectors at the designated pressure. To simulate this fault, the pressure sensor of the fuel pump was disconnected (Fig. S6).

g) Fuel injector

The high pressure fuel injector delivers the required amount of diesel fuel into each cylinder at the designated pressure to achieve fine spray atomisation and evaporation processes. The injector is an electromechanical device that controls the injection duration and timing. The resistance of the electrical system is made to a tightly specified tolerance so the response of the injector is repeatable and reliable. To simulate failure, one of the injectors was disconnected (Fig. S7). This resulted in inconsistent fuel injection between cylinders.

h) Injector sealing

To simulate this failure, an injector with a damaged sealing surface was installed which could affect the fuel spray condition (Fig. S8).

2.2.3. Exhaust after-treatment system

i) DOC blockage

DOC converts diesel pollutant emissions to harmless products by oxidation processes of reactions (1-3) [28, 29]. CO and HC emissions are oxidized into CO_2 and H_2O, while NO is oxidized into NO_2 which needs further treatment. The malfunction was simulated by using a used and blocked DOC filter (Fig. S9). Testing with a blocked DOC may impact the emissions and fuel consumption performance.

$$C_3H_6 + 4.5O_2 \rightarrow 3CO_2 + 3H_2O \quad (1)$$

$$CO + 0.5O_2 \rightarrow CO_2 \quad (2)$$

$$NO + 0.5O_2 \rightarrow NO_2 \quad (3)$$

j) SCR

SCR converts NO and NO_2 emissions to N_2 and H_2O in a lean diesel exhaust environment with the aid of catalyst and reductant through the mechanisms of reactions (4-6) [29]. In this study, the reductant is ammonia (NH_3) carried in Adblue. To simulate the SCR malfunction, the Adblue level in the storage tank was drained to a low warning level (Fig. S10), which would affect the injection of Adblue. Insufficient injection would result in low conversion efficiency of NO and NO_2, while over injection would cause undesirable NH_3 emissions to the atmosphere [30].

$$\text{Standard SCR: } 4NH_3 + 4NO + O_2 \rightarrow 4N_2 + 6H_2O \quad (4)$$

$$\text{Fast SCR: } 4NH_3 + 2NO + 2NO_2 \rightarrow 4N_2 + 6H_2O \quad (5)$$

$$NO_2 \text{ SCR: } 4NH_3 + 3NO_2 \rightarrow 3.5N_2 + 6H_2O \quad (6)$$

k) DPF blockage

A DPF removes particulate emissions when the diesel exhaust gas flows by its honeycomb wall-flow monolith filter and burns off the accumulated particulates regularly (regeneration) [31]. The DPF malfunction was simulated by a used and blocked filter (Fig. S11). Testing with a blocked DPF will increase the exhaust back pressure and reduce the power of the engine. Furthermore, it may also impact the reduction efficiency of the particulate emissions.

l) DPF pressure sensor

A DPF pressure sensor monitors the exhaust pressure difference across the inlet and outlet of the filter, which is used to determine the amount of soot captured and then to trigger the DPF regeneration [32]. The malfunction was simulated by disconnecting the DPF pressure sensor (Fig. S12). In this state, regeneration would be affected and the particulate emissions will accumulate within the porous microstructure of the filter wall. As a result, the DPF will be blocked once the mileage has been achieved.

m) NO_x sensor

The NO_x sensor measures the concentrations of NO_x in the exhaust and provides information to the SCR system to adjust the injection rate of Adblue [33]. The malfunction was simulated by disconnecting the whole NO_x sensor (Fig. S13). In this state, the injection rate of Adblue may be affected, resulting in low reduction efficiency of NO_x emissions. Modern trucks may suffer power limitations if NO_x emission levels do not meet the standard [34].

n) AdBlue injector

The Adblue injector is designed to inject the optimal NH_3 dosing into the exhaust stream of the SCR system for the maximum NO_x reduction [35, 36]. The malfunction was simulated by disconnecting the injection control cable (Fig. S14). In this state, the injector would not inject any AdBlue dosing into the exhaust stream and the deNO_x performance would be impacted.

2.2.4. Other faults

o) Thermostat fully open

The thermostat controls the coolant flow to maintain the engine temperature at an optimal operating level. The thermostat operates on a sealed chamber containing a wax pellet that melts and expands at a set temperature. The malfunction was simulated by using a fully open thermostat (Fig. S15). When this occurs, the engine would always lose heat to the radiator and thus operate at a lower temperature, which would influence the fuel consumption and emissions performance.

p) Oil pump

The oil pump circulates engine oil to lubricate the sliding components to reduce friction, wear and temperature, including the bearings, pistons and camshaft [37]. The malfunction was simulated by disconnecting the pressure sensor of the oil pump. When this occurs, the warning light of low oil pressure is on (Fig. S16) and the engine will be able to run but it will not be as well as controlled. This could lead to further vehicle damage if the engine is keep operating in a certain period of time.

3. Results and discussion

The experimental results will be presented and discussed in two sub-sections, the effect of engine malfunctions on fuel consumption and CO_2 emissions, and on gaseous criteria emissions. The effect of malfunctions on engine performance is evaluated against the baseline test with all the engine and emission control systems functioning properly.

3.1. Fuel consumption and CO_2 emissions

Figs. 2 and 3 show the effect of simulated engine malfunctions on the fuel consumption rate (L/100 km) and CO_2 emission factor (g/km) of the truck. For a production engine, the combustion efficiency is relatively high and most of the carbon in the fuel is converted into CO_2. Therefore, the fuel consumption rate and CO_2 emission factor generally show the same variations. As shown in Figs. 2 and 3, it is obvious that all the malfunctions increase the fuel consumption rate and CO_2 emission factor except for the fault of EGR fully closed. When the EGR valve is fully closed, the fuel consumption rate actually decreases significantly by 31% from 34.48 (baseline) to 23.74 L/100 km (EGR fully closed). This is because more oxygen can be inducted into the combustion chamber for a better combustion process when EGR is fully closed [38]. In addition, the heat capacity of the in-cylinder gas will be reduced without the extra CO_2 and H_2O from EGR, leading to higher pressure rise, larger power output and thus lower fuel consumption [39]. For the same reasons, the fuel consumption rate is increased by 16% when EGR is fully open (maximum EGR) compared to the baseline test.

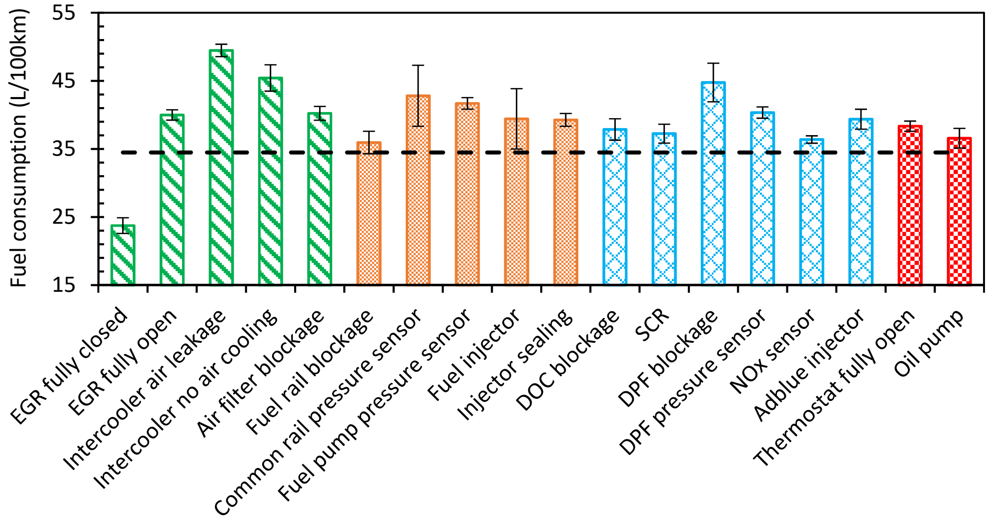

Fig. 2. Effect of engine malfunctions on fuel consumption. Error bars indicate standard deviations and dashed line indicates fuel consumption of the baseline test with all engine and emission control systems working properly.

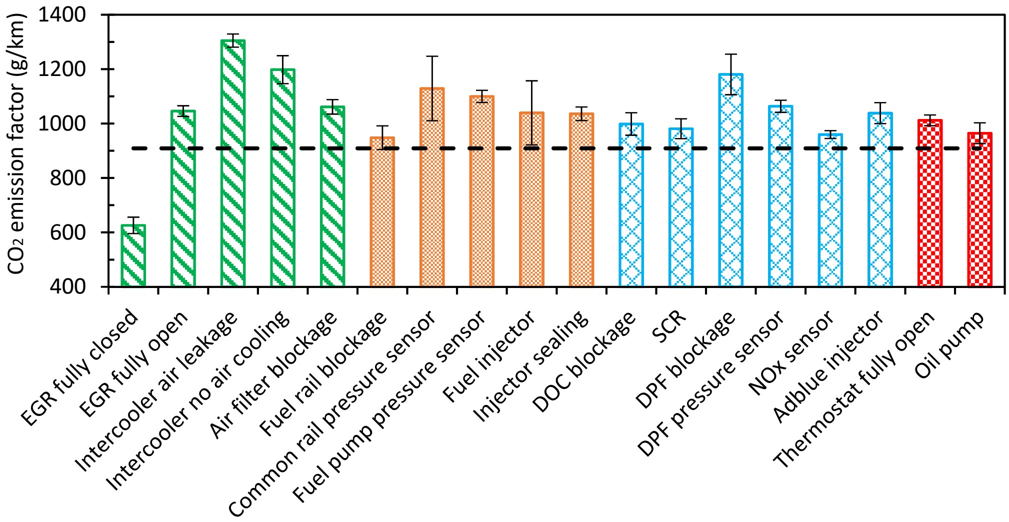

Fig. 3. Effect of engine malfunctions on CO_2 emission factors. Error bars indicate standard deviations and dashed line indicates emission factor of the baseline test with all engine and emission control systems working properly.

The biggest increases (17%-43%) in fuel consumption are caused the malfunctions in the intake system, with 43% by intercooler air leakage, 32% by intercooler no air cooling and 17% by air filter blockage. The intercooler is designed to cool the charge air after the turbocharger and EGR, aiming to increase the volumetric efficiency, engine power and knock limits and to reduce the emissions and thermal stress [40]. With air leakage or no air cooling in the intercooler, the charge density could be decreased significantly, which would then proportionally reduce the mean effective pressure and hence lead to higher fuel consumption rate [41]. Similarly, with a blocked air filter, the volumetric efficiency and intake pressure would be decreased, leading to higher pumping loss and fuel consumption rate.

The second biggest increases (6%-30%) in fuel consumption rates are caused by the faults in the exhaust after-treatment system. Among them, DPF blockage and DPF pressure sensor faults cause 30% and 17% of increases in fuel consumption, respectively. This may be caused by the increased exhaust back pressure, which increases exhaust residual in the cylinder (internal EGR) and deteriorates combustion quality. In addition, higher exhaust back pressure reduces the volumetric efficiency and increases the pumping loss. Consequently, the fuel consumption rate is increased. For similar reasons, DOC blockage also increases fuel consumption by 10%. Unexpectedly, malfunctions of the NO_x control devices increase fuel consumption noticeably, with 14% by Adblue injector, 8% by SCR and 6% by NO_x sensor. This may be because the ECU of modern diesel engines switches operation to the default mode when there is a fault in the NO_x after-treatment system. This change limits the power of the engine [34] and thus increases the fuel consumption.

The malfunctions in the fuel injection system could also cause remarkable increases (4%-24%) in fuel consumption: common rail pressure sensor (24%), fuel pump pressure sensor (21%), fuel injector (14%), injector sealing (14%) and fuel rail blockage (4%). The CRDI system provides accurate and flexible control of injection pressure, timing and duration to achieve the optimal fuel spray atomization, evaporation, mixing and combustion processes. It is a key technology to achieve the required power, torque, emissions and fuel economy performance. However, these simulated faults affect the designed injection pressure or duration, resulting in deteriorated combustion quality (e.g. longer ignition delay, lower combustion speed and incomplete combustion) and thus higher fuel consumption.

Finally, other malfunctions cause moderate increases in fuel consumption, with 11% by thermostat and 6% by engine oil pump. The fault of thermostat fully open causes extra heat loss and low (non-optimal) coolant temperature for engine operation, and the fault of oil pump causes higher friction loss. As a result, both faults could lead to worsened fuel economy.

3.2. Pollutant emissions

The European emission standards for heavy-duty diesel vehicles (> 3.5 tonnes) are defined in g/kW-h measured on engine dynamometers, which are different to that of light-duty diesel vehicles in g/km measured on chassis dynamometers. This is because chassis dynamometer testing of heavy-duty vehicles is expensive and type approval of one engine model using an engine dynamometer will enable its use for many vehicle models powered by the same engine model. In this study, the emission factors derived from chassis dynamometer testing are in g/km. To convert emission factors from g/kW-h to g/km, several parameters are needed including the vehicle fuel economy factor (23.74 L/100km, baseline test in Fig. 2), fuel density (832 g/L), fuel heating value (45.5 MJ/kg) and engine thermal efficiency. The overall engine brake thermal efficiency is assumed to be 35% based on experimental results from similar heavy duty diesel engines [2, 16, 42]. Using the above values, 1 g/kW-h corresponds to 0.87 g/km (meaning that 1 km driving distance consumes about 0.87 kW-h engine work). Therefore, the Euro VI transient limits [4] are 0.14, 3.48 and 0.40 g/km for HC, CO and NOx emissions, respectively.

Figs. 4 and 5 show the effect of engine malfunctions on the HC and CO emission factors, respectively. Generally, HC and CO emission factors are relatively low due to the mechanism of diesel's non-premixed lean combustion. Even with all these simulated malfunctions, the HC and CO emission factors could still remain well below the Euro VI limits except for CO with the faults of EGR fully open. Moreover, the effect of a faulty sensor or component on HC and CO emissions is insignificant in most cases. For HC, as shown in Fig. 4, the emission factors are unchanged or even slightly reduced for 12 out of the 18 simulated malfunctions. For CO, as shown Fig. 5, the emission factors are un-changed or even significantly reduced for 16 out of the 18 malfunctions. This is explainable as the emission control system for diesel vehicles is mostly focused on NO and PM emissions reduction. There would be some trade-offs between NO/PM and CO/HC emissions, so that the deactivation/removal of the some emission control device would actually reduce CO/HC emissions but increase the NO emissions. This has been demonstrated by Fig. 6 which shows that the NO emission factors generally have the opposite trends as CO/HC emissions.

The largest increases in HC and CO emission factors are caused by EGR fully open which increases HC by 3.4 times and CO by 11.2 times. This is mainly because HC and CO are products of unburnt or incomplete combustion. With EGR fully open, there would be too much exhaust gas (CO_2) recirculated back into the combustion chamber, which dilutes the oxygen and causes incomplete combustion. Other faults that cause noticeable increases in HC are intercooler air leakage (146%), fuel pump pressure sensor (99%) and common rail pressure sensor (98%). The only other fault that causes increase in CO is in the SCR (133%). It is interesting to notice that the SCR fault increases CO (+133%) and HC (+9%) but not very much in NO (+38%), while DOC fault increases NO (+197%) but decreases CO (-37%) and HC (-13%). This seems to be conflicting with the major functions of SCR (for NO control) and DOC (for CO and HC control). As explained above, this may be caused by the correction of ECU which detects the faults and then runs the engine in a default mode. The increase/decrease in CO and HC indicates fuel enrichment/leanness in the combustion zone, leading to lowered/increased NO formation in the combustion chamber. Such enrichment/leanness could be caused by ECU default mode under SCR/DOC fault.

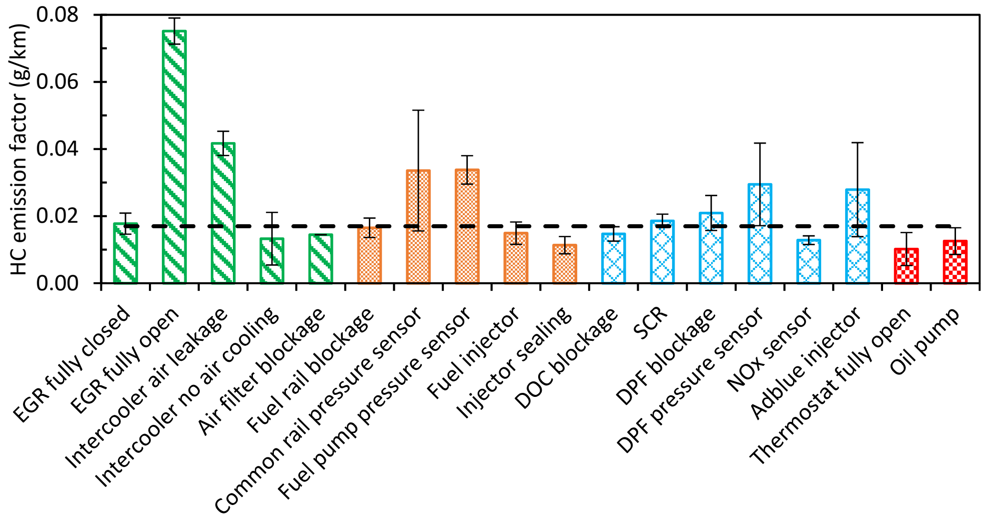

Fig. 4. Effect of engine malfunctions on HC emission factors. Error bars indicate standard deviations and dashed line indicates emission factor of the baseline test with all engine and emission control systems working properly.

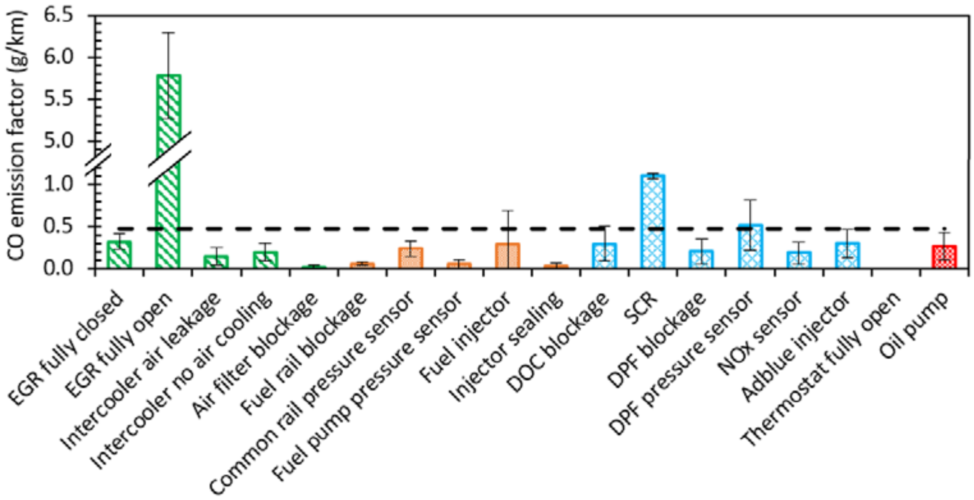

Fig. 5. Effect of engine malfunctions on CO emission factors. Error bars indicate standard deviations and dashed line indicates emission factor of the baseline test with all engine and emission control systems working properly.

Fig. 6 shows the effect of engine malfunctions on NO emission factors. The large error bars indicate that the engine control and exhaust after-treatment devices are running roughly and unstably when these malfunctions occur. Opposite to the trends observed for HC and CO, NO emission factors are increased significantly by many of the malfunctions. Three of the simulated faults could increase NO by more than ten times, namely DPF pressure sensor (16.1 times), Adblue injector (16.0 times) and fuel pump pressure sensor (12.6 times). Another five faults cause NO to increase by four to ten times, including common rail pressure sensor (9.2 times), DPF blockage (8.4 times), fuel injector (7.4 times), intercooler no air cooling (6.0 times) and intercooler air leakage (4.4 times).

Unacceptably high roadside NO_2 concentration is a major air pollution problem in cities worldwide [26, 43] and diesel vehicles are a major source of NO_x emissions in urban areas [44]. Fig. 6 shows clearly that properly functioning of the after-treatment and fuel injection systems is of great importance for achieving the expected NO_x emission standards. The main function of SCR is to convert NO_x to N_2 with the aid of a catalyst and reductant (i.e. Adblue as NH_3 source in this study) [19]. With a fault in the Adblue injector, NO emission factors could be increased by 16.0 times. The pressure difference across the DPF could also significantly affect NO emission factors. With a fault in the DPF pressure sensor or DPF blockage, the NO emission factors increase by 16.1 or 8.4 times. This may be because these two faults result in high or wrong signals of pressure difference across the DPF, which trigger unnecessary active regeneration events of DPF filter [15, 45]. Active regeneration uses high temperature (550 ℃ or higher) to oxidise the soot accumulated in DPF filter, which could reduce the NO_x reduction efficiency of urea-based SCR system due to the largely oxidised ammonia, reduced oxygen concentration, thermal deactivation of SCR catalyst, and poisoning of SCR catalyst by HC emissions [45].

Besides after-treatment devices, in-cylinder combustion optimisation is another key technology for controlling NO emissions. Fig. 6 shows that four faults in the fuel injection system could increase NO emission factors by 7.4-12.6 times. High-pressure CRDI is an important approach to achieve the strict Euro 5/V-6/VI standards of diesel engines [4]. The faults in the injector, fuel pump and pressure sensor of the CRDI system would have changed the optimised diesel combustion process via injection pressure, timing or duration, and consequently increased the NO formation. The two intercooler faults (i.e. air leakage and no air cooling) also cause remarkable increases (4.4-6.0 times) in NO emission factors. With air leakage or no air cooling in the intercooler, the intake air temperature increases, leading to higher combustion temperature and consequently higher NO emissions [46, 47].

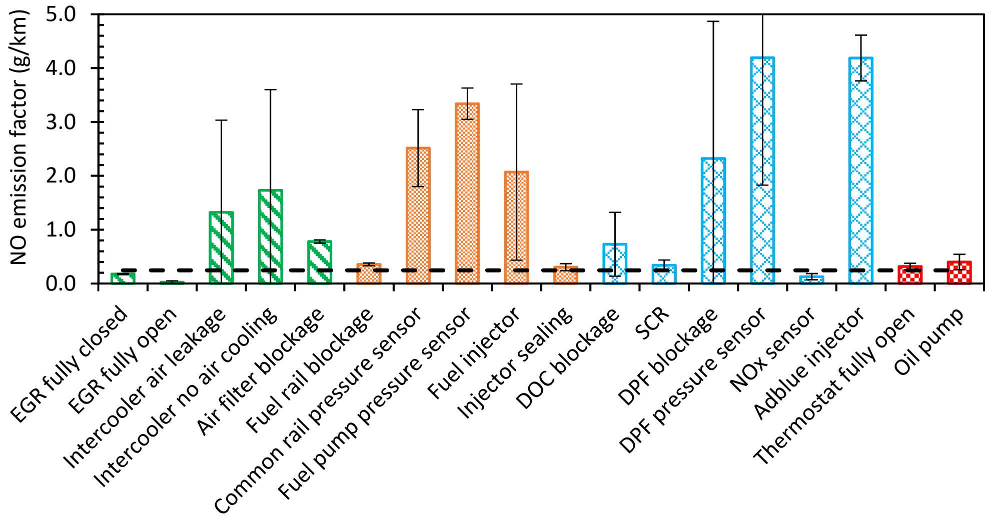

Fig. 6. Effect of engine malfunctions on NO emission factors. Error bars indicate standard deviations and dashed line indicates emission factor of the baseline test with all engine and emission control systems working properly.

Fig. 6 also shows that three faults could reduce NO emission factors noticeably. In particular, EGR fully open could reduce NO by 90% compared to the baseline tests. This is because, with the maximum EGR rate, the in-cylinder combustion temperature and oxygen concentration are greatly reduced, which limits the formation of thermal NO [48]. However, EGR fully closed and NO sensor faults could reduce NO emission factors by 28% and 48%, respectively. For the NO sensor fault, the ECU could detect it and then have urea dosing in default mode and thus still have lower NO. For the case of EGR fully closed, the NO emissions are driving mode related. Second by second experimental data (Fig. 7) shows that the tests with EGR fully closed actually have higher NO concentrations than baseline tests under acceleration, but not under other conditions which have longer time and distance (thus larger weighting factor). As a result, the cycle integrated NO emission factor of EGR fully closed is slightly lower than that of baseline test.

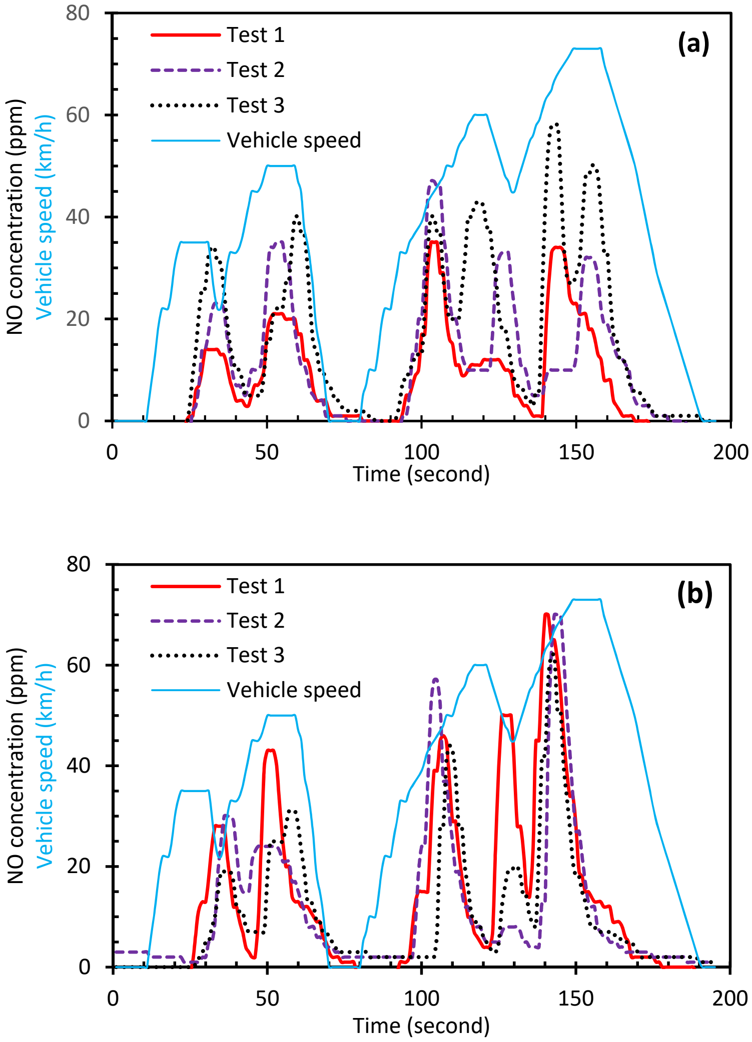

Fig. 7. NO emission concentrations of baseline (a) and EGR fully closed (b) tests.

4. Conclusions

This study comprehensively investigated the effect of various engine malfunctions on fuel consumption and gaseous emissions performance of a Euro VI diesel truck using transient chassis dynamometer testing. The simulated malfunctions included those that would commonly occur in the intake, fuel injection and exhaust after-treatment systems. The effect of malfunctions on engine performance was evaluated against the baseline tests with all the engine and emission control systems functioning properly. This study demonstrated clearly the significance of proper functioning of engine control and exhaust after-treatment systems to achieve the required performance of fuel consumption and pollutant emissions. The major results are summarised as follows:

(1) All the simulated engine malfunctions increased fuel consumption and CO_2 emission factor except for EGR fully closed which reduced fuel consumption by 31% compared to baseline tests. The biggest increases in fuel consumption were caused by malfunctions in the intake system, ranging from 16% by EGR fully open to 43% by intercooler air leakage. This was followed by malfunctions in the exhaust after-treatment (6%-30%) and fuel injection (4%-24%) systems. Malfunctions in other system also caused moderate increases in fuel consumption, with 11% by thermostat and 6% by engine oil pump.

(2) The effect of engine malfunctions on HC and CO emission factors was insignificant in most cases. HC and CO emission factors could remain unchanged or even reduced for most of the simulated malfunctions. The largest increases were caused by EGR fully open (maximum EGR which resulted in incomplete combustion), with HC and CO increased by 3.4 and 11.2 times, respectively.

(3) The effect of engine malfunctions on NO emission factors was generally opposite to HC and CO emission factors and the effect was significant. The largest increases were caused by malfunctions in the exhaust after-treatment system, in particular Adblue injector (16.0

times), DPF pressure sensor (16.1 times) and DPF blockage (8.4 times). Malfunctions in fuel injection system increased NO greatly, ranging from 24% by common rail injector sealing to 12.6 times by fuel pump pressure sensor. Intercooler malfunctions also increased NO noticeably, with 6.0 times by no air cooling and 4.4 times by air leakage.

Acknowledgement

This project was funded by the Environmental Protection Department of the Hong Kong Special Administrative Region (SAR) Government, Hong Kong China. The contents of this paper are solely the responsibility of the authors and do not necessarily represent official views of the Hong Kong SAR Government.

References

[1] N.A. Ramlan, W.J. Yahya, A.M. Ithnin, *et al.*, Performance and emissions of light-duty diesel vehicle fuelled with non-surfactant low grade diesel emulsion compared with a high grade diesel in Malaysia. *Energy Convers Manage* 2016; 130: 192-199.

[2] H. Liu, J. Ma, F. Dong, *et al.*, Experimental investigation of the effects of diesel fuel properties on combustion and emissions on a multi-cylinder heavy-duty diesel engine. *Energy Convers Manage* 2018; 171: 1787-1800.

[3] F. Posada, Z. Yang, R. Muncrief, Review of Current Practices and New Developments in Heavy-Duty Vehicle Inspection and Maintenance Programs, *The International Council on Clean Transportation*, 2015.

[4] M. Williams, R. Minjares, A technical summary of Euro 6/VI vehicle emission standards, *The International Council on Clean Transportation*, 2016.

[5] Y. Huang, B. Organ, J.L. Zhou, *et al.*, Remote sensing of on-road vehicle emissions: Mechanism, applications and a case study from Hong Kong. *Atmos Environ* 2018; 182: 58-74.

[6] European Commission, EU action to curb air pollution by cars: Questions and Answers (MEMO/17/2821), *European Commission - Fact Sheet*, 2017.

[7] F. Fung, B. Suen, Improving Hong Kong's Emission Inspection Programme for On-road Diesel Commercial Vehicles, *Civic Exchange*, 2014.

[8] D. Zhao, E. Winward, Z. Yang, *et al.*, Characterisation, control, and energy management of electrified turbocharged diesel engines. *Energy Convers Manage* 2017; 135: 416-433.

[9] A. Grönman, P. Sallinen, J. Honkatukia, *et al.*, Design and experiments of two-stage intercooled electrically assisted turbocharger. *Energy Convers Manage* 2016; 111: 115-124.

[10] K. Nanthagopal, B. Ashok, R.T. Karuppa Raj, Influence of fuel injection pressures on Calophyllum inophyllum methyl ester fuelled direct injection diesel engine. *Energy Convers Manage* 2016; 116: 165-173.

[11] A.K. Agarwal, A. Dhar, J.G. Gupta, *et al.*, Effect of fuel injection pressure and injection timing of Karanja biodiesel blends on fuel spray, engine performance, emissions and combustion characteristics. *Energy Convers Manage* 2015; 91: 302-314.

[12] B. Rajesh Kumar, S. Saravanan, D. Rana, *et al.*, Combined effect of injection timing and exhaust gas recirculation (EGR) on performance and emissions of a DI diesel engine fuelled with next-generation advanced biofuel – diesel blends using response surface methodology. *Energy Convers Manage* 2016; 123: 470-486.

[13] D. Damodharan, A.P. Sathiyagnanam, D. Rana, *et al.*, Combined influence of injection timing and EGR on combustion, performance and emissions of DI diesel engine fueled with neat waste plastic oil. *Energy Convers Manage* 2018; 161: 294-305.

[14] S. Wang, X. Zhu, L.M.T. Somers, *et al.*, Effects of exhaust gas recirculation at various loads on diesel engine performance and exhaust particle size distribution using four blends with a research octane number of 70 and diesel. *Energy Convers Manage* 2017; 149: 918-927.

[15] D. Buono, A. Senatore, M.V. Prati, Particulate filter behaviour of a Diesel engine fueled with biodiesel. *Appl Therm Eng* 2012; 49: 147-153.

[16] S. Ren, B. Wang, J. Zhang, *et al.*, Application of dual-fuel combustion over the full operating map in a heavy-duty multi-cylinder engine with reduced compression ratio and diesel oxidation catalyst. *Energy Convers Manage* 2018; 166: 1-12.

[17] J.M. Luján, H. Climent, L.M. García-Cuevas, *et al.*, Pollutant emissions and diesel oxidation catalyst performance at low ambient temperatures in transient load conditions. *Appl Therm Eng* 2018; 129: 1527-1537.

[18] C.P. Cho, Y.D. Pyo, J.Y. Jang, *et al.*, NOx reduction and N2O emissions in a diesel engine exhaust using Fe-zeolite and vanadium based SCR catalysts. *Appl Therm Eng* 2017; 110: 18-24.

[19] B. Guan, R. Zhan, H. Lin, *et al.*, Review of state of the art technologies of selective catalytic reduction of NOx from diesel engine exhaust. *Appl Therm Eng* 2014; 66: 395-414.

[20] A.J. Hickman, Vehicle maintenance and exhaust emissions. *Sci Total Environ* 1994; 146-147: 235-243.

[21] C.L. Chase, C.L. Peterson, G.A. Lowe, *et al.*, A 322,000 kilometer (200,000 mile) Over the Road Test with HySEE Biodiesel in a Heavy Duty Truck. *SAE Paper 2000-01-2647*, 2000.

[22] R.L. McCormick, M.S. Graboski, T.L. Alleman, *et al.*, Quantifying the Emission Benefits of Opacity Testing and Repair of Heavy-Duty Diesel Vehicles. *Environ Sci Technol* 2003; 37: 630-637.

[23] J. Huang, L. Lin, Y. Wang, *et al.*, Experimental study of the performance and emission characteristics of diesel engine using direct and indirect injection systems and different fuels. *Fuel Process Technol* 2011; 92: 1380-1386.

[24] J. Kowalski, An experimental study of emission and combustion characteristics of marine diesel engine with fuel pump malfunctions. *Appl Therm Eng* 2014; 65: 469-476.

[25] HKEPD, Strengthened Emissions Control for Petrol and LPG Vehicles, 2018, http://www.epd.gov.hk/epd/english/environmentinhk/air/guide_ref/remote_sensing_Petrol_n_LPG.htm <accessed 06.04.2018>.

[26] Y. Huang, Y.S. Yam, C.K.C. Lee, *et al.*, Tackling nitric oxide emissions from dominant diesel vehicle models using on-road remote sensing technology. *Environ Pollut* 2018; 243: 1177-1185.

[27] UNECE, Regulation No 83 of the Economic Commission for Europe of the United Nations (UNECE) - Uniform provisions concerning the approval of vehicles with regard

to the emission of pollutants according to engine fuel requirements [2015/1038]. *Official Journal of the European Union* 2015; 172: 1-249.

[28] A.P. Triana, J.H. Johnson, S.L. Yang, *et al.*, An Experimental and Numerical Study of the Performance Characteristics of the Diesel Oxidation Catalyst in a Continuously Regenerating Particulate Filter. *SAE paper 2003-01-3176*, 2003.

[29] A. Russell, W.S. Epling, Diesel Oxidation Catalysts. *Catal Rev* 2011; 53: 337-423.

[30] M. Nahavandi, Selective catalytic reduction (SCR) of NO by ammonia over V2O5/TiO2 catalyst in a catalytic filter medium and honeycomb reactor: a kinetic modeling study. *Braz J Chem Eng* 2015; 32: 875-893.

[31] F. Payri, A. Broatch, J.R. Serrano, *et al.*, Experimental–theoretical methodology for determination of inertial pressure drop distribution and pore structure properties in wall-flow diesel particulate filters (DPFs). *Energy* 2011; 36: 6731-6744.

[32] K.G. Rappé, Integrated Selective Catalytic Reduction–Diesel Particulate Filter Aftertreatment: Insights into Pressure Drop, NOx Conversion, and Passive Soot Oxidation Behavior. *Ind Eng Chem Res* 2014; 53: 17547-17557.

[33] C. Quérel, A. Bonfils, O. Grondin, *et al.*, Control of a SCR system using a virtual NOx sensor. *IFAC Proc Vol* 2013; 46: 9-14.

[34] R.B. Gurung, T. Lindgren, H. Boström, Predicting NOx sensor failure in heavy duty trucks using histogram-based random forests. *Int J Progno Health Manag* 2017; 8: 1-14.

[35] S.-J. Jeong, S.-J. Lee, W.-S. Kim, Numerical Study on the Optimum Injection of Urea–Water Solution for SCR DeNOx System of a Heavy-Duty Diesel Engine to Improve DeNOx Performance and Reduce NH3 Slip. *Environ Eng Sci* 2008; 25: 1017-1036.

[36] İ.A. Reşitoğlu, K. Altinişik, A. Keskin, The pollutant emissions from diesel-engine vehicles and exhaust aftertreatment systems. *Clean Technol Environ Policy* 2015; 17: 15-27.

[37] D.Q. Truong, K.K. Ahn, N.T. Trung, *et al.*, Performance analysis of a variable-displacement vane-type oil pump for engine lubrication using a complete mathematical model. *Proc Inst Mech Eng D* 2013; 227: 1414-1430.

[38] R. Schubiger, A. Bertola, K. Boulouchos, Influence of EGR on Combustion and Exhaust Emissions of Heavy Duty DI-Diesel Engines Equipped with Common-Rail Injection Systems. *SAE paper 2001-01-3497*, 2001.

[39] D. De Serio, A. de Oliveira, J.R. Sodré, Effects of EGR rate on performance and emissions of a diesel power generator fueled by B7. *J Braz Soc Mech Sci Eng* 2017; 39: 1919-1927.

[40] J. Barman, P. Ghodke, J. Joseph, Evaluation of Intercooler Efficiency as a Technique for Reducing Diesel Engine Emissions. *SAE paper 2011-01-1133*, 2011.

[41] R.v. Basshuysen, F. Schäfer. Internal Combustion Engine Handbook - Basics, Components, System, and Perspectives (2nd Edition). SAE International.

[42] D. Singh, S.K. Singal, M.O. Garg, *et al.*, Transient performance and emission characteristics of a heavy-duty diesel engine fuelled with microalga Chlorella variabilis and Jatropha curcas biodiesels. *Energy Convers Manage* 2015; 106: 892-900.

[43] S.K. Grange, A.C. Lewis, S.J. Moller, *et al.*, Lower vehicular primary emissions of NO2 in Europe than assumed in policy projections. *Nat Geosci* 2017; 10: 914-918.

[44] S.C. Anenberg, J. Miller, R. Minjares, *et al.*, Impacts and mitigation of excess diesel-related NOx emissions in 11 major vehicle markets. *Nature* 2017; 545: 467-471.

[45] P. Chen, J. Wang, Air-fraction modeling for simultaneous Diesel engine NOx and PM emissions control during active DPF regenerations. *Appl Energy* 2014; 122: 310-320.

[46] A. Pal, M. V, S. Gupta, *et al.*, Performance and Emission Characteristics of Isobutanol-Diesel Blend in Water Cooled CI Engine Employing EGR with EGR Intercooler. *SAE paper 2013-24-0151*, 2013.

[47] J. Shen, J. Qin, M. Yao, Turbocharged diesel/CNG Dual-fuel Engines with Intercooler: Combustion, Emissions and Performance. *SAE paper 2003-01-3082*, 2003.

[48] Y. Huang, G. Hong, R. Huang, Numerical investigation to the dual-fuel spray combustion process in an ethanol direct injection plus gasoline port injection (EDI + GPI) engine. *Energy Convers Manage* 2015; 92: 275-286.

Supporting information

Fig. S1. EGR valve in the engine (left) and faulty EGR valves (right).

Fig. S2. Intercooler air leakage (left) and no air cooling (right).

Fig. S3. Clean and blocked air filters.

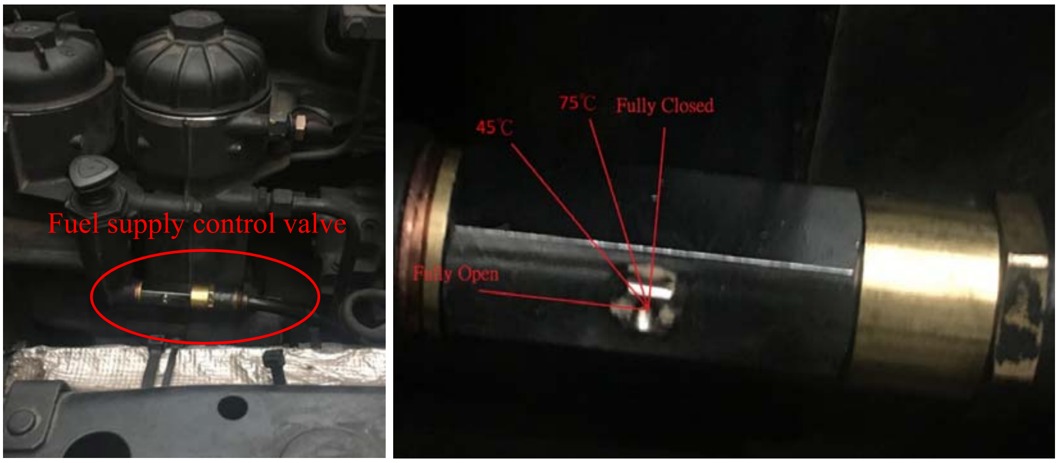

Fig. S4. Simulation of fail rail blockage.

Fig. S5. Disconnection of fuel rail pressure sensor.

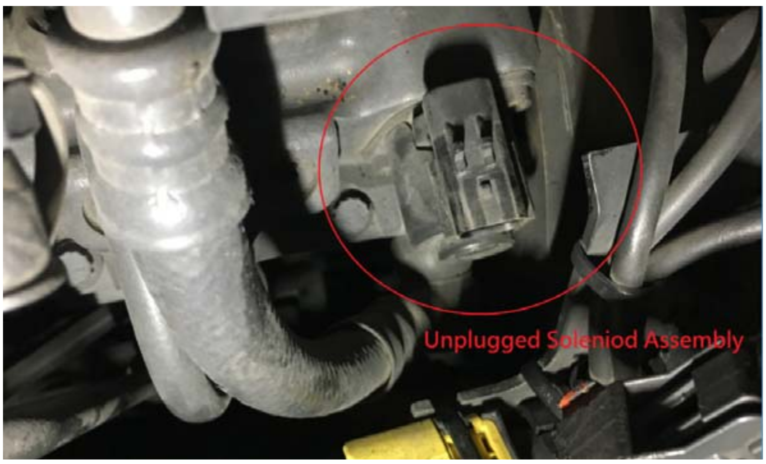

Fig. S6. Disconnection of fuel pump pressure sensor.

Fig. S7. Disconnection of one injector.

Fig. S8. Installation of an injector with a damaged sealing surface.

Fig. S9. The inlet side of DOC (left) and the clean and blocked DOC filters (right).

Fig. S10. Adblue was drained to a warning level on the dashboard.

Fig. S11. Blocked (left) and clean (right) DPF filters.

Fig. S12. Disconnected DPF pressure sensor.

Fig. S13. Disconnected NO_x sensor.

Fig. S14. Disconnected AdBlue injector control cable.

Fig. S15. Fully open (left) and sealed (right) thermostats.

Fig. S16. Warning light of low oil pressure on the dashboard.